Ionic Liquids Hot Paper

How to cite: *Angew. Chem. Int. Ed.* **2020**, *59*, 14429–14433
International Edition: doi.org/10.1002/anie.202005991
German Edition: doi.org/10.1002/ange.202005991

On the Dynamic Interaction of *n*-Butane with Imidazolium-Based Ionic Liquids

*Radha G. Bhuin, Leonhard Winter, Matthias Lexow, Florian Maier, and Hans-Peter Steinrück**

Abstract: *The impact of a reactant from the gas phase on the surface of a liquid and its transfer through this gas/liquid interface are crucial for various concepts applying ionic liquids (ILs) in catalysis. We investigated the first step of the adsorption dynamics of n-butane on a series of 1-alkyl-3-methylimidazolium bis(trifluoromethanesulfonyl)imide ILs ($[C_nC_1Im][Tf_2N]$; $n = 1, 2, 3, 8$). Using a supersonic molecular beam in ultra-high vacuum, the trapping of n-butane on the frozen ILs was determined as a function of surface temperature, between 90 and 125 K. On the C_8- and C_3-ILs, n-butane adsorbs at 90 K with an initial trapping probability of ≈ 0.89. The adsorption energy increases with increasing length of the IL alkyl chain, whereas the ionic headgroups seem to interact only weakly with n-butane. The absence of adsorption on the C_1- and C_2-ILs is attributed to a too short residence time on the IL surface to form nuclei for condensation even at 90 K.*

The catalytic conversion of hydrocarbons is a key process of the chemical industry, for example, for the production of commodity chemicals or polymers. In this context, two important catalytic concepts have been introduced.[1] Both utilize ionic liquids (ILs), which are salts typically with melting points below 100 °C[2] and often an extremely low vapor pressure.[3] ILs can be tailored over a wide range, and thus are an important class of liquid materials for many applications.[1c,4] The two catalytic concepts are supported ionic liquid phase (SILP)[1a,d] catalysis and solid catalyst with ionic liquid layer (SCILL).[1b] In both, a thin IL layer coats the catalyst support. The reactants enter from the gas phase through the gas/liquid interface, react with the dissolved catalyst complex in SILP or with the IL-modified solid catalyst in SCILL, and the formed products are released again through the gas/liquid interface. Thus, the transfer of gas molecules through this interface is crucial in both concepts. Despite the importance of ILs in catalysis, the dynamics of the adsorption of reactants at the gas/IL interface and its dependence on the interface properties have hardly been studied in detail so far. Previous studies concern the adsorption/desorption and state-resolved scattering experiments of small molecules.[5]

Upon impact of a gas molecule onto an IL, it exchanges energy and momentum with the moieties in the topmost IL layer. This situation corresponds to the interaction of molecules with solid surfaces, which has been studied using supersonic molecular beams under ultra-high vacuum (UHV) conditions in detail in the past. Using this approach, the trapping of physisorbed species (or the sticking of chemisorbed species) have been determined on a variety of metal surfaces.[6] The trapping (or sticking) probability, S, is defined as ratio of the adsorption rate R_{ads} and the impingement rate R_{imp} of molecules on the surface, $S = R_{ads}/R_{imp}$.[6a,e] S depends on the properties of the surface (temperature, composition, adsorbate coverage) and of the incoming molecules (kinetic and internal energy, angle of incidence, orientation).[6a]

In this study, we address the interaction of *n*-butane with a series of 1-alkyl-3-methylimidazolium bis(trifluoromethanesulfonyl)imide ILs, $[C_nC_1Im][Tf_2N]$ ($C_n = C_1$, C_2, C_3, C_8), which we denote as C_n-ILs in the following. *n*-Butane is considered as a model system for a number of important catalytic processes, for example, refinery alkylation reactions,[7] hydroformylations[1a] and hydrogenations of alkenes.[1b] In addition, investigations on single crystal metal surfaces can serve as reference systems. By studying ILs with different lengths of the alkyl chain, we aim in particular for an understanding of the role of the alkyl chain as compared to the ionic groups.

The dynamic interaction of an incoming molecule with an IL depends on the interaction potential. For hydrocarbons, the interaction potential is a sum of weak attractive van-der-Waals forces and strong short-range Pauli repulsion. The resulting well-depth is only shallow, such that no stable adsorption occurs at room temperature (RT).[6a] In order to obtain information on trapping probabilities and adsorption energies, we thus have to work at conditions, where stable adsorption of *n*-butane on the IL occurs. This cannot be achieved at RT, but requires temperatures below 100 K. Notably, at this temperature, ILs are not in their liquid state, but are frozen. Nevertheless, we expect that the surface structures in the liquid and in the frozen states are quite similar, since many ILs form amorphous solids upon cooling. For the C_8-IL, we verified this for thin IL films by temperature-dependent angle-resolved X-ray photoelectron spectroscopy (ARXPS, see Figure S1 and S2 of the Supporting Information). We are therefore confident that we can transfer our conclusions also to the liquid state at or above RT.

[*] Dr. R. G. Bhuin, L. Winter, Dr. M. Lexow, Dr. F. Maier, Prof. Dr. H.-P. Steinrück
Lehrstuhl für Physikalische Chemie 2, Friedrich-Alexander-Universität Erlangen-Nürnberg
Egerlandstr. 3, 91058 Erlangen (Germany)
E-mail: hans-peter.steinrueck@fau.de

Supporting information and the ORCID identification number(s) for the author(s) of this article can be found under: https://doi.org/10.1002/anie.202005991.

To determine the trapping probabilities of *n*-butane on the different ILs, we used a newly built three-stage supersonic molecular beam setup with a quadrupole mass spectrometer (QMS), which is combined with an X-ray photoelectron spectrometer (XPS). In contrast to common supersonic beam setups with a horizontal beam, our beam impinges on the surface vertically from the top, to be able to study horizontally mounted liquid samples. The ultraclean ILs (as checked by XPS) were spread on a polycrystalline Ni support ($12\times 12\,mm^2$, Goodfellow), which can be cooled with liquid N_2 down to 88 K. The temperature is measured by a K-type thermocouple, which is inserted into a small hole at the side of the Ni support. The thickness of the IL films was ≈ 1 mm.

The trapping probabilities were determined using the well-established direct method by King and Wells,[8] which uses two flags to control the molecular beam: The beam flag inside the molecular beam setup allows us to switch the beam on and off. The sample flag in the analysis chamber can be positioned such that the molecular beam can impinge or not impinge on the sample.

In Figure 1, two series of trapping probability measurements of *n*-butane on the C_8- and C_3-IL are depicted, for temperatures from 90 to 118 K. To explain the King and Wells method,[8] we discuss the data at 90 and 102 K for the C_8-IL. The Figure shows the partial pressure of *n*-butane ($m/z=43$) in the chamber, as measured by QMS, versus time. At $t=-40$ s, the beam flag and the sample flag are closed, which yields a zero *n*-butane signal (after background subtraction). At $t=-20$ s, the beam flag is opened, leading to a sudden signal increase, $\Delta p_{beam,}$ in the analysis chamber. The closed sample flag prevents the beam from hitting the sample at this time. At $t=0$ s, the sample flag is removed so that the beam hits the sample, which induces a pronounced signal drop, Δp_{ads}, by $\approx 90\,\%$. This drop is due to the fact that molecules adsorb on the sample and thus are not detected by the QMS (if all molecules would adsorb, the *n*-butane signal would go back to zero, that is, the sample would act like a perfect pump). From this initial drop, we determine the initial trapping probability S_0 (at zero *n*-butane coverage on the IL) as the ratio of the signal drop at $t=0$ s devided by the

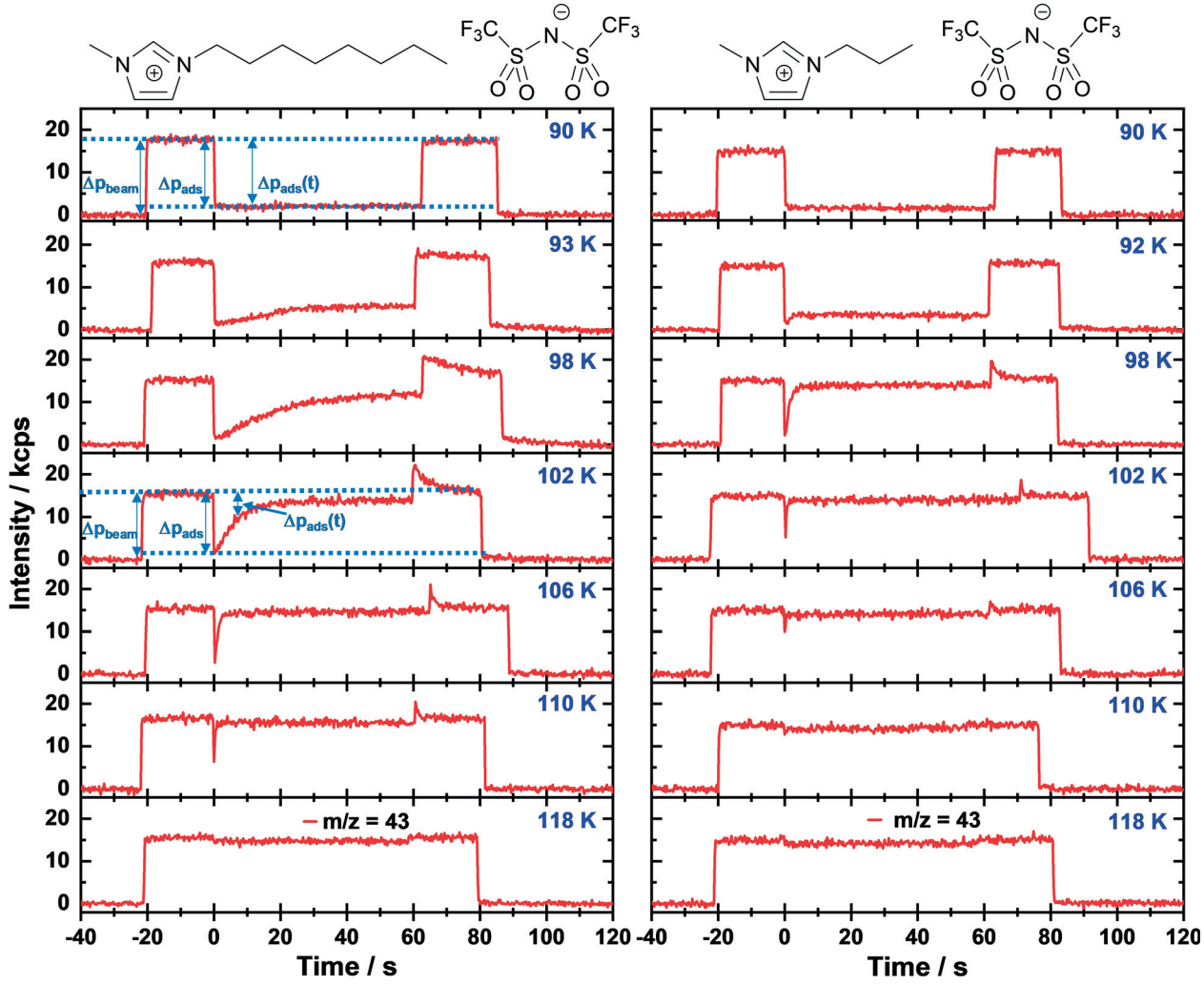

Figure 1. Trapping probability measurements of *n*-butane on $[C_8C_1Im][Tf_2N]$ (left) and $[C_3C_1Im][Tf_2N]$ (right) at selected temperatures. The *n*-butane partial pressure was monitored using $m/z=43$, which is the most intense fragment. A linear background was subtracted from all curves. The kinetic energy of the unseeded *n*-butane beam with the nozzle at RT is estimated to be 13 kJ mol^{-1}, by comparison to ref. [12].

signal increase at $t = -20$ s, that is, $S_0 = R_{ads}/R_{imp} = \Delta p_{ads}/\Delta p_{beam}$.

With increasing time, the signal stays constant (90 K) or increases again (102 K), which reflects the time-dependent trapping probability $S(t) = \Delta p_{ads}(t)/\Delta p_{beam}$. The time dependence follows from the fact that with time *n*-butane accumulates on the IL surface, which can influence the trapping behavior. With the knowledge of the beam flux, the time dependence can be converted into a coverage dependence (see below).

At $t \approx 60$ s (depending on the individual experiment), the sample flag is closed. At 90 K, the pressure increases back to the value before opening the sample flag, as one would expect. At 102 K, the increase is even larger, and after the sudden increase the signal decreases exponentially to the value before opening the sample flag; this effect will be addressed below. Finally at ≈ 80 s, the beam flag is also closed and the *n*-butane signal drops back to zero.

We first address the initial trapping probability S_0 (at zero coverage) on the C_8-IL as a function of IL temperature, as plotted in Figure 2 (red circles). At 90 K, we observe a value of 0.89 ± 0.03. S_0 stays constant up to ≈ 102 K and then drops to zero. At the characteristic temperature $T_{50\%}$ (C_8) = 110 K, S_0 has dropped to 50 % of its initial value. We attribute this decrease of S_0 above ≈ 102 K not to a change of the probability of getting adsorbed on the surface, but to the concomitant onset of desorption from the adsorbed layer. If desorption is fast compared to the measurement time of the first data point (0.30 s), one obtains an apparently smaller value of S_0. Thus, $T_{50\%}$ contains valuable information on the desorption energy (see below).

For the C_3-IL, we observe a very similar behavior in Figure 2 (blue triangles), albeit shifted to lower temperature by 6 K: The initial S_0 value of 0.88 ± 0.03 is constant until ≈ 96 K and then drops to zero with $T_{50\%}$ (C_3) = 104 K. Interestingly, for the C_1- and C_2-ILs (green diamonds and purple triangles in Figure 2) no trapping is observed even at the lowest temperature of 88 K. For comparison, we also plotted a measurement series on clean Ni(111), that is, without an IL (black squares). While the initial trapping probability is identical, 0.88 ± 0.04 at 90 K, it stays constant up to ≈ 135 K, and decreases thereafter with $T_{50\%}$ (Ni) = 150 K. Our data clearly show that the interaction with *n*-butane depends on the length of the alkyl chain of the IL. The $T_{50\%}$ values are 110 K for the C_8-IL, 104 K for the C_3-IL, and values to small to be measured for the C_2- and C_1-ILs. Using the $T_{50\%}$ values, we can determine information on the differences in desorption energy of *n*-butane on the different ILs (see below).

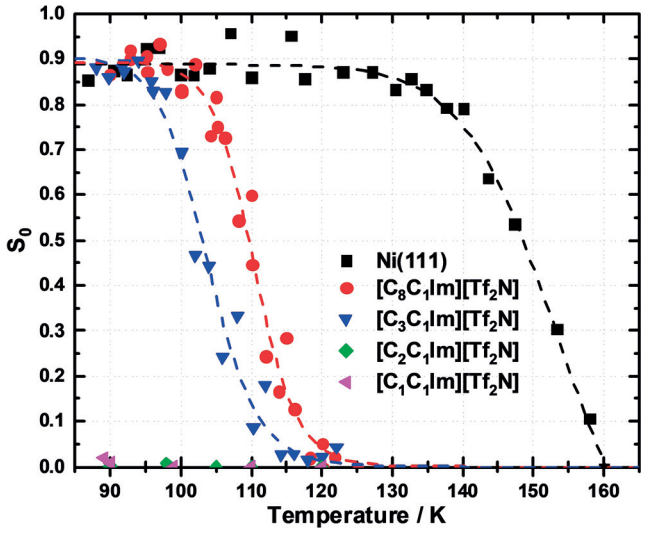

Figure 2. Temperature-dependent initial trapping probability of *n*-butane on [C_nC_1Im][Tf_2N] ILs with varying chain length compared to the initial trapping probability on Ni(111). The dashed lines are guides to the eye.

Next, we discuss the time dependence of the trapping probabilities $S(t)$ in Figure 1. For the C_8-IL, the *n*-butane signal at 90 K remains unchanged after the initial drop at $t = 0$ s, until the sample flag is closed at $t \approx 60$ s. This indicates negligible desorption, and that after saturation of the first layer, *n*-butane multilayers continue to adsorb with the same trapping probability. At higher temperatures, the signal increases after the initial drop at $t = 0$ s, and this increase becomes more pronounced with increasing temperature. This is due to the fact that the desorption rate now is not negligible any more, but rather is proportional to the coverage, which increases until the first layer is filled. It levels off either when the (higher) desorption rate of the multilayer at this temperature is reached (from 93 to 98 K) or when the pressure value before opening the sample flag is reached, which indicates identical desorption and adsorption rates (that is, zero "net" trapping). After switching off the beam at $t \approx 60$ s, the pressure increases to values above those before opening the sample flag. This behavior is due to the fact that now the adsorption flux is turned off, but desorption still occurs. This differential signal decays exponentially.

In Figure 3 a, we show the "net" trapping probability, $S^*(\theta)$, on the C_8-IL as a function of coverage for temperatures up to 106 K. While $S(\theta)$ solely describes the trapping probability into the adsorbed state, $S^*(\theta)$ also accounts for possible desorption, at given coverage θ. For all temperatures above 90 K, we initially observe a linear decrease of $S^*(\theta)$, which in a simple picture can be understood in the following way: We assume that $S(\theta)$ is independent of coverage (which is the case at 90 K; see Figure 3 a). Then the adsorption rate is $R_{ads} = S(\theta) \cdot R_{imp} = S_0 \cdot R_{imp}$ (with $R_{imp} = 2.0 \times 10^{13}$ molecules $cm^{-2} s^{-1}$). With time, the coverage $\theta = \int (R_{ads} - R_{des})\, dt$ builds up on the surface. While the desorption rate is zero at 90 K, at higher temperature significant desorption starts counteracting adsorption, with a rate $R_{des} = \theta \cdot \nu \cdot \exp(-E_{des}/RT)$, leading to a decrease of $S^*(\theta)$. If the desorption energy E_{des} does not depend on coverage, the desorption rate increases linearly with coverage, which explains the linear decrease of $S^*(\theta)$ in Figure 3 a. In a next step, the slopes of this decrease for different temperatures are analyzed in an Arrhenius plot in Figure 3 b. From a linear fit, we obtain a desorption energy of 29 ± 3 kJ mol^{-1} and a prefactor of $1.4 \times 10^{14 \pm 2}$ s^{-1}.

For the C_3-IL, we observe an overall similar behavior as for the C_8-IL, albeit shifted to lower temperatures (compare data at 106 K for the C_8-IL and 98 K for the C_3-IL in Figure 1). In Figure S3 of the Supporting Information, we show the

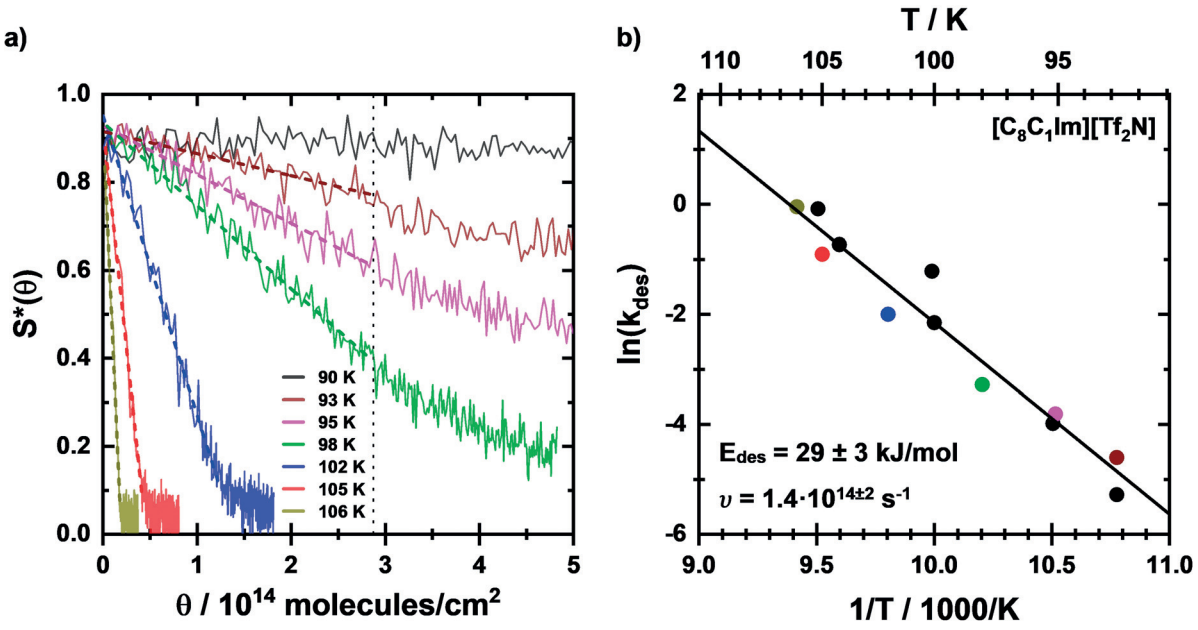

Figure 3. (a) Net trapping probability of *n*-butane on $[C_8C_1Im][Tf_2N]$ as a function of coverage for various temperatures. The behavior is fitted linearly (dashed lines). (b) Arrhenius analysis of the rate constants k_{des} obtained from (a). From the linear fit, the desorption energy and the pre-exponential factor are derived; colored symbols in (b) correspond to the colored curves in (a). The coverage of a closed monolayer is indicated by a vertical dotted line in (a). It was determined assuming that the saturation coverage on Ni(111) at 102 K corresponds to that of a freestanding layer of flat-lying *n*-butane, that is, 2.87×10^{14} molecules cm^{-2}, as taken from ref. [13].

"net" trapping probability, $S^*(\theta)$, also for the C_3-IL as a function of coverage. In this case, however, the accessible temperature range is too small for an Arrhenius analysis. However, we can use the shift of $T_{50\%}$ in Figure 2 by 6 K to lower temperatures to estimate the difference in desorption energy compared to the C_8-IL. Using the same prefactor, a decrease of the desorption energy by $\approx 6\%$ explains the observed shift.

To understand the absence of any trapping on the C_2- and C_1-ILs, we have to consider that *n*-butane multilayers on the C_8- and C_3-ILs start to desorb with an onset just above 90 K. The fact that we observe constant S_0 values of ≈ 0.89 up to 102 and 95 K on the C_8- and C_3-IL, respectively, indicates that *n*-butane molecules are stronger bound to these two ILs than in the multilayer; otherwise desorption would immediately occur. For the C_2- and C_1-ILs, the adsorption energy is smaller than the condensation energy, and individual molecules immediately desorb after adsorption, such that we measure a zero value for S_0.

In a simplified picture, the surface of the investigated ILs is composed of the $[Tf_2N]^-$ anion with the CF_3 groups pointing outwards,[9] the imidazolium headgroup, and the non-polar alkyl chains of the cation.[10] The absence of trapping on the C_1- and C_2-ILs at 88 K (that is, where *n*-butane condenses in multilayers on other surfaces) indicates that the attractive van-der-Waals forces between *n*-butane and the polar head groups and also with the C_1- and C_2-chains are too weak. Only upon increasing the alkyl chain length, we observe trapping, which indicates that starting from the C_3-IL, the attractive interaction between *n*-butane and the alkyl chain is strong enough for permanent adsorption on the surface. For the C_8-IL, the interaction is even stronger; here, also the well-known alkyl surface enrichment for chains with $n \geq 4$ will contribute.[9,11]

An interesting point to be addressed is the reason why we observe multilayer formation of *n*-butane on the C_8- and C_3-ILs up to 95 K, but not on the C_2- and C_1-ILs. We attribute this observation to the fact that nuclei are required for multilayer growth. The formation of stable nuclei needs, however, a certain coverage on the surface, so that statistically enough molecules encounter each other. Due to the weak interaction with the C_2- and C_1-ILs, the residence time of *n*-butane on these surfaces is too short to form such stable nuclei. We tried to increase the beam flux by a factor of 10, and also extended the exposure time to 900 s, but did not observe any adsorption.

Interestingly, a similar effect was observed in thermal desorption studies for water adsorbed on frozen $[C_8C_1Im][BF_4]$ and $[C_2C_1Im][Tf_2N]$, where the desorption energies of the monolayers were found to be smaller than for the multilayer, along with a vanishing initial trapping probability below the multilayer desorption temperature.[5f] This is in line with the behavior observed here for *n*-butane on C_1- and C_2-ILs, where no trapping was observed either. For water on the two ILs, an observed increase of the trapping probability with coverage was attributed to dominating adsorbate-adsorbate interactions.[5f] This effect was not observed here, which is assigned to the too short residence time for the formation of a nucleus. It is also noteworthy to mention that state-resolved scattering experiments on the same ILs as studied here showed that the sticking probabilities of NO are not influenced by the alkyl chain length for low kinetic energies, in line with our results for *n*-butane.[5a]

In conclusion, we studied the trapping of *n*-butane on different $[C_nC_1Im][Tf_2N]$ ILs ($n = 1, 2, 3, 8$) using a supersonic molecular beam at low temperatures. From the initial trapping probability at zero *n*-butane coverage, we deduce that the adsorption energy on the ILs increases with increasing chain length. On the C_8- and C_3-ILs, we find pronounced trapping while on the C_2- and C_1-ILs no trapping occurs. We thus conclude that the adsorption energy of *n*-butane on the IL surface is dominated by the interaction with the alkyl chain, while the interaction with the ionic head groups seems much weaker. One interesting observation is that at 88 K on the C_2- and C_1-ILs multilayer formation is suppressed, despite the fact that it occurs on the C_8- and C_3-ILs and also on Ni(111) even at significantly higher temperatures. This is attributed to the absence of nucleus formation due to a too short residence time. We believe that the conclusions derived from our UHV experiments at low temperature on frozen amorphous ILs can be transferred to ILs in their liquid phase at room temperature or above, because the first impact of a molecule from the gas phase determines the energy and momentum transfer with the liquid. Since the interaction strength increases with increasing chain length, using ILs with longer alkyl chains should increase the efficiency of this first step. The well-known surface enrichment of longer alkyl chains could even enhance this effect.

Acknowledgements

R.B., L.W., M.L. and H.-P.S. thank the European Research Council (ERC) under the European Union's Horizon 2020 research and innovation programme for financial support, in the context of the Advanced Investigator Grant "ILID" to H.-P.S. (Grant Agreement No. 693398-ILID). We acknowledge the support by Bernd Kreß, Hans-Peter Bäumler and the mechanical workshop, when planning and assembling the new UHV setup.

Conflict of interest

The authors declare no conflict of interest.

Keywords: gas-surface dynamics · ionic liquids · molecular beam · *n*-butane · trapping and adsorption

[1] a) C. P. Mehnert, R. A. Cook, N. C. Dispenziere, M. Afeworki, *J. Am. Chem. Soc.* **2002**, *124*, 12932 – 12933; b) U. Kernchen, B. Etzold, W. Korth, A. Jess, *Chem. Eng. Technol.* **2007**, *30*, 985 – 994; c) H.-P. Steinrück, P. Wasserscheid, *Catal. Lett.* **2015**, *145*, 380 – 397; d) A. Riisager, R. Fehrmann, M. Haumann, B. S. K. Gorle, P. Wasserscheid, *Ind. Eng. Chem. Res.* **2005**, *44*, 9853 – 9859; e) S. Walter, M. Haumann, P. Wasserscheid, H. Hahn, R. Franke, *AIChE J.* **2015**, *61*, 893 – 897; f) T. Barth, W. Korth, A. Jess, *Chem. Eng. Technol.* **2017**, *40*, 395 – 404.

[2] "Ionic Liquids in Synthesis": *Ionic Liq. Synth.*, 2nd ed. (Eds.: P. Wasserscheid, T. Welton), Wiley-VCH, Weinheim, **2008**.

[3] a) P. Wasserscheid, *Nature* **2006**, *439*, 797; b) M. J. Earle, J. M. S. S. Esperança, M. A. Gilea, J. N. Canongia Lopes, L. P. N. Rebelo, J. W. Magee, K. R. Seddon, J. A. Widegren, *Nature* **2006**, *439*, 831 – 834.

[4] N. V. Plechkova, K. R. Seddon, *Chem. Soc. Rev.* **2008**, *37*, 123 – 150.

[5] a) A. Zutz, D. J. Nesbitt, *AIP Adv.* **2016**, *6*, 105207; b) X. Li, G. C. Schatz, D. J. Nesbitt, *J. Phys. Chem. B* **2012**, *116*, 3587 – 3602; c) J. R. Roscioli, D. J. Nesbitt, *J. Phys. Chem. Lett.* **2010**, *1*, 674 – 678; d) M. Buckley, K. L. Syres, R. G. Jones, *Faraday Discuss.* **2018**, *206*, 475 – 495; e) S. G. Hessey, R. G. Jones, *Chem. Sci.* **2013**, *4*, 2519 – 2529; f) A. Deyko, R. G. Jones, *Faraday Discuss.* **2012**, *154*, 265 – 288.

[6] a) J. F. Weaver, A. F. Carlsson, R. J. Madix, *Surf. Sci. Rep.* **2003**, *50*, 107 – 199; b) C.-L. Kao, R. J. Madix, *Surf. Sci.* **2004**, *557*, 215 – 230; c) C. R. Henry, *Surf. Sci. Rep.* **1998**, *31*, 231 – 325; d) S. L. Bernasek, *Adv. Chem. Phys.* **1980**, *41*, 477 – 516; e) J. A. Barker, D. J. Auerbach, *Surf. Sci. Rep.* **1984**, *4*, 1 – 99; f) C. R. Arumainayagam, R. J. Madix, *Prog. Surf. Sci.* **1991**, *38*, 1 – 102.

[7] C.-P. Huang, Z.-C. Liu, C.-M. Xu, B.-H. Chen, Y.-F. Liu, *Appl. Catal. A* **2004**, *277*, 41 – 43.

[8] D. A. King, M. G. Wells, *Surf. Sci.* **1972**, *29*, 454 – 482.

[9] K. R. J. Lovelock, C. Kolbeck, T. Cremer, N. Paape, P. S. Schulz, P. Wasserscheid, F. Maier, H.-P. Steinrück, *J. Phys. Chem. B* **2009**, *113*, 2854 – 2864.

[10] a) C. Waring, P. A. J. Bagot, J. M. Slattery, M. L. Costen, K. G. McKendrick, *J. Phys. Chem. A* **2010**, *114*, 4896 – 4904; b) M. A. Tesa-Serrate, B. C. Marshall, E. J. Smoll, S. M. Purcell, M. L. Costen, J. M. Slattery, T. K. Minton, K. G. McKendrick, *J. Phys. Chem. C* **2015**, *119*, 5491 – 5505.

[11] K. Shimizu, B. S. J. Heller, F. Maier, H.-P. Steinrück, J. N. Canongia Lopes, *Langmuir* **2018**, *34*, 4408 – 4416.

[12] A. V. Hamza, H.-P. Steinrück, R. J. Madix, *J. Chem. Phys.* **1986**, *85*, 7494 – 7495.

[13] K. Lee, Y. Morikawa, D. C. Langreth, *Phys. Rev. B* **2010**, *82*, 155461.

Manuscript received: April 25, 2020
Revised manuscript received: May 18, 2020
Accepted manuscript online: May 19, 2020
Version of record online: July 1, 2020

